

Renormalized perturbation theory at large expansion orders

Riccardo Rossi¹, Fedor Šimkovic^{2,3} IV, and Michel Ferrero^{2,3}

¹*Center for Computational Quantum Physics, Flatiron Institute, 162 5th Avenue, New York, NY 10010*

²*CPHT, CNRS, Ecole Polytechnique, Institut Polytechnique de Paris, Route de Saclay, 91128 Palaiseau, France*

³*Collège de France, 11 place Marcelin Berthelot, 75005 Paris, France*

(Dated: January 27, 2020)

We present a general formalism that allows for the computation of large-order renormalized expansions in the spacetime representation, effectively doubling the numerically attainable perturbation order of renormalized Feynman diagrams. We show that this formulation compares advantageously to the currently standard techniques due to its high efficiency, simplicity, and broad range of applicability. Our formalism permits to easily complement perturbation theory with non-perturbative information, which we illustrate by implementing expansions renormalized by the addition of a gap or the inclusion of Dynamical Mean-Field Theory. As a result, we present numerically-exact results for the square-lattice Fermi-Hubbard model in the low temperature non-Fermi-liquid regime and show the momentum-dependent suppression of fermionic excitations in the antinodal region.

Renormalization is one of the most fruitful ideas in physics. Originally discovered as a method to eliminate one-loop Feynman-diagram infinities in quantum electrodynamics (QED) [1–4], it has notably led to one of the most precise comparisons of theory and experiment [5]. The usefulness of renormalization beyond high-energy physics has soon been understood and it was applied to condensed matter physics [6, 7] and especially to the theory of critical phenomena [8], which has led to the development of the perturbative renormalization group technique. As computing renormalized Feynman diagrams is at the core of our quantitative understanding of nature, it is of critical importance to find efficient strategies in order to successfully perform computations. Yet, evaluating a large number of diagram orders is an extremely challenging task even with modern computational facilities. For example, no 6-loop QED computation has been attempted to date, despite strong interest due to the availability of high-precision experiments. The main limitation in computing large-order contributions is the “factorial barrier” represented by the factorial growth of the number of Feynman diagrams with increasing diagram order. The Diagrammatic Monte Carlo algorithm [9–13] was introduced with the idea that Feynman diagrams could be good sampling variables in strongly-correlated electronic systems as they can be defined directly in the thermodynamic and continuum limit. While this approach dramatically simplified and automatized the computation of Feynman diagrams, and there are many recent advancements in this direction [14–19], it is still limited by the factorial barrier as it considers explicit Feynman diagram topologies.

A recently introduced algorithm overcomes the factorial barrier by computing connected and irreducible bare Feynman diagrams [20–23] at a computational cost growing exponentially with expansion order, which allowed for the computation of an unprecedented number of Feynman-diagram orders directly in the thermodynamic limit. Similarly effective exponential algorithms

overcoming the factorial barrier have also been found for the real-time evolution of quantum systems [24–27], allowing to reach the large-time limit in quantum impurity models.

While bare expansions are remarkably powerful for fermionic systems on a lattice and at finite temperatures [14, 22, 28, 29], given the finite radius of convergence and the resulting polynomial complexity of the many-body problem [30], they are nevertheless limited by the appearance of poles in the complex plane. These poles may prohibit the resummation of the series in vicinity of sharp crossovers [22]. Moreover, in the very-low temperature regime infrared divergencies are generically present [31]. Renormalization is the fundamental missing tool to continue to make progress. For example, it has been shown that optimized chemical potential shifts can already yield drastic improvements to the properties of evaluated series [14, 32]. Furthermore, when considering systems directly in the continuous space, one is generally forced to perform renormalization from the start in order to be able to even define the theory.

In this Letter, we present a general formalism that allows for the numerical computation of renormalized perturbative expansions at large expansion orders. More precisely, we prove that it is possible to overcome the factorial barrier: We compute factorially-many renormalized Feynman diagrams in the spacetime representation with only an exponential cost, independently of the renormalization procedure. In what follows, we introduce the underlying theoretical concepts and show examples of large order computations, up to 10 – 14 orders, for the square-lattice Fermi-Hubbard model in non-perturbative regimes, where no other controlled techniques are applicable. To achieve this goal we have designed new renormalization schemes using non-perturbative information, such as approximate solutions from Dynamical Mean-Field Theory (DMFT [33]), altering the bare series in a way that extends the convergence radius and the applicability of perturbation theory. Finally, we show that the

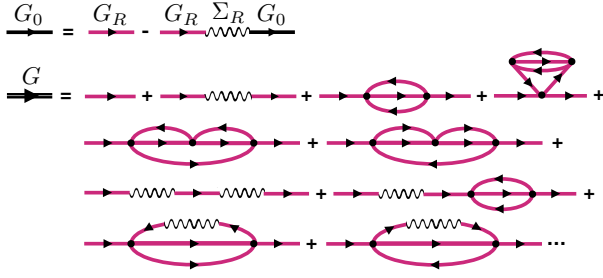


FIG. 1. Quadratic self-energy renormalization. Top: Dyson-like equation relating the bare Green's function $G_0[\xi]$, the renormalized Green's function G_R and the self-energy functional $\Sigma_R[\xi]$. Bottom: explicit examples of diagrams contributing to the physical Green's function $G[\xi]$.

renormalized expansion can be used in the non-Fermi-liquid regime of the Hubbard model by computing the spectral function, which shows a strong suppression of antinodal quasiparticles.

For concreteness, we focus our discussion on one-particle renormalizations for the Hubbard model in the following theoretical part. We introduce a generalization of the “shifted action” of Ref. [34]

$$S_{\text{bare}}[G_0, \xi] = -\langle \varphi | G_0^{-1} | \varphi \rangle + \int_X \xi(X) (\bar{\varphi}_\uparrow \bar{\varphi}_\downarrow \varphi_\downarrow \varphi_\uparrow)(X), \quad (1)$$

where φ_σ is a Grassmann field, X is the imaginary-time-lattice coordinate, and $\xi(X)$ is a spacetime dependent coupling constant. The expansion in powers of ξ reproduces exactly the bare expansion in the spacetime representation. For example, the Green's function

$$G[\xi](Y, Y') := -\frac{\int e^{-S_{\text{bare}}[G_0, \xi]} \varphi(Y) \bar{\varphi}(Y')}{\int e^{-S_{\text{bare}}[G_0, \xi]}} \quad (2)$$

can be written as

$$G[\xi](Y, Y') = \sum_{n=0}^{\infty} \frac{1}{n!} \int_{1, \dots, n} G_{Y, Y'}(\{X_1, \dots, X_n\}) \prod_{j=1}^n \xi(X_j), \quad (3)$$

where the functional derivative with respect to $\xi(X_j)$, $G_{Y, Y'}(\{X_1, \dots, X_n\})$, is the sum of all connected bare Feynman diagrams with $X_1 \dots X_n$ as internal vertex positions, symmetrized with respect to permutations of the internal vertices, and with Y and Y' as external points. One-particle renormalization in the spacetime representation can be achieved by substituting G_0 with a functional of the interaction ξ , which we denote by $\tilde{G}_0[\xi]$

$$(\tilde{G}_0[\xi])^{-1} =: G_R^{-1} + \Sigma_R[\xi]. \quad (4)$$

The functional $\tilde{G}_0[\xi]$ is equal to an arbitrary G_R at zero interaction, and it coincides with the physical bare propagator G_0 for $\xi(X) = U$, at the value of the interaction

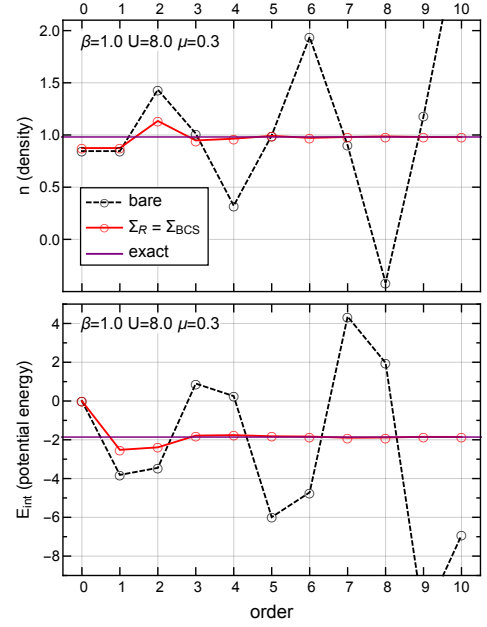


FIG. 2. Partial sums of the bare series (dashed black lines) and BCS-shifted series (red lines) for Hubbard atom density (top plot) and potential energy (bottom plot) are compared to analytic results (purple lines).

strength U we are interested in. There are no restrictions on the functional $\Sigma_R[\xi]$, in particular it can be defined as an infinite series in ξ without computational overhead. We can now define the renormalized action functional as

$$S_R[G_R, \xi] := S_{\text{bare}}[G_0[\xi], \xi] \quad (5)$$

and use it to define the Green's function as the ξ functional

$$G[\xi](Y, Y') := -\frac{\int e^{-S_R[G_R, \xi]} \varphi(Y) \bar{\varphi}(Y')}{\int e^{-S_R[G_R, \xi]}}. \quad (6)$$

The sum of all renormalized Feynman diagrams for fixed symmetrized spacetime positions is then obtained by expanding in powers of ξ . $G_{Y, Y'}(\{X_1, \dots, X_n\})$ from Eq. (3) is now the sum of all symmetrized renormalized Feynman diagrams with internal vertex positions X_1, \dots, X_n . For example, the fully-renormalized one-particle scheme, also called “bold”, is obtained by imposing that $\Sigma_R[\xi]$ is such that $G[\xi](Y, Y')$ is a constant functional identically equal to G_R : $G[\xi] = G_R$. In this case, $\Sigma_R[\xi]$ can be diagrammatically constructed as the sum of all two-particle irreducible, “bold”, diagrams. Not all renormalization schemes have a simple Feynman-diagrammatic interpretation: renormalization using Feynman diagrams becomes quickly unmanageable with order in the general case as one has to keep track of all possible counter-terms.

A key observation is that Eq. (5) implies that renormalized expansions are equivalent to bare expansions with a

functional propagator $\tilde{G}_0[\xi]$. We can therefore apply the CDet algorithm [20] for bare expansions, provided we can generalize it to functionals. We introduce an efficient and general way to deal with functional expansions based on “nilpotent polynomials”, functions of n commuting symbols z_j such that $z_j^2 = 0$, for $j \in \{1, \dots, n\}$. If we want to compute n -th order functional derivatives with respect to $\xi(X_1) \dots \xi(X_n)$, we only need to expand the functional up to linear order in each $\xi(X_j) =: z_j$, $j \in \{1, \dots, n\}$, discarding any term of order z_j^2 and higher. Nilpotent polynomials of n variables form a ring, where multiplication is defined as a subset convolution, which can be performed in $O(3^n)$ operations, or alternatively $O(n^2 2^n)$ operations using a fast subset convolution [35]:

$$\begin{aligned} Q_3(z_1, \dots, z_n) &= Q_1(z_1, \dots, z_n) \cdot Q_2(z_1, \dots, z_n) \\ \iff Q_3(V) &= \sum_{S \subseteq V} Q_1(S) Q_2(V \setminus S), \end{aligned}$$

where $Q_i(V)$ is the coefficient of $\prod_{j \in V} z_j$. Interestingly, the recursive formula from Ref. [20] which is used to compute sums of connected diagrams for the bare expansion based on $S_{\text{bare}}[G_0, \xi]$ can be reinterpreted as polynomial division between two nilpotent polynomials [23]:

$$\begin{aligned} Q_3(z_1, \dots, z_n) &= Q_1(z_1, \dots, z_n) / Q_2(z_1, \dots, z_n) \\ \iff Q_3(V) &= Q_1(V) - \sum_{S \subsetneq V} Q_3(S) Q_2(V \setminus S), \end{aligned}$$

where $Q_2(\emptyset) = 1$ is assumed. We can therefore obtain a fast algorithm for renormalized expansions by considering a nilpotent-polynomial-valued bare propagator $\tilde{G}_0(z_1, \dots, z_n)$ and use the CDet algorithm. For fermionic systems we need to compute the sum of determinants of nilpotent-polynomial matrices, a task that can be performed using additions, multiplications, and divisions of nilpotent polynomials. One can show that the computational cost to compute the sum of all symmetrized renormalized Feynman diagrams for fermionic systems for a given configuration of interaction vertices is $O(n^3 4^n)$, or alternatively $O(n^5 3^n)$ by using fast subset convolutions [36], much better than $(n!)^2$ which is a lower bound on the cost of enumerating all diagrams over all permutations of internal vertices.

We now focus our attention on the Fermi-Hubbard model on the square lattice, defined by the Hamiltonian

$$\hat{H} = - \sum_{i,j,\sigma} t_{ij} \hat{\psi}_{\sigma i}^\dagger \hat{\psi}_{\sigma j} + U \sum_i \hat{\psi}_{\uparrow i}^\dagger \hat{\psi}_{\downarrow i}^\dagger \hat{\psi}_{\downarrow i} \hat{\psi}_{\uparrow i}, \quad (7)$$

where i, j are lattice sites, $t_{ij} = 1$ for nearest neighbors, $t_{ij} = t'$ for next-nearest neighbors, and zero otherwise. We are interested in the repulsive model where $U > 0$ with an average number of particles per site n close to one. In the regime of low temperatures and/or high interactions the bare expansion becomes very difficult to

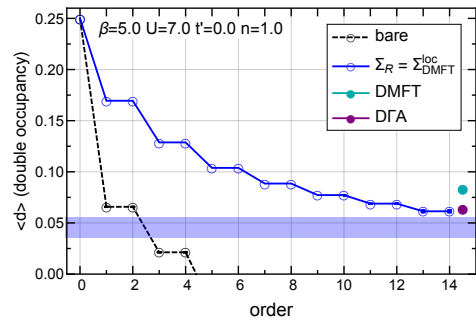


FIG. 3. Partial sums for the double occupancy for the half-filled Hubbard model. The bare series (dashed black lines) and the DMFT-shifted series (blue lines) and the resummed result for the DMFT-shifted series (Padé approximants, horizontal blue line) are shown. The double occupancy from DMFT (green) and a linear DGA extrapolation (purple) are plotted for comparison (data courtesy of T. Schäfer).

compute and evaluate, seemingly due to infrared divergencies coming from shifts of the non-interacting Fermi surface. Moreover, the presence of a superfluid instability in the attractive model ($U < 0$) reduces the radius of convergence of the series to zero at zero temperature.

Two main renormalization approaches have been proposed to cure the bare expansion: The first is a fully self-consistent (bold) formalism which eliminates infrared divergencies by using the physical propagator in the expansion [13]. However, a known problem with this approach is that the bold scheme can converge towards unphysical answers at strong interactions [37, 38]. A second approach is a renormalized perturbation theory at fixed Fermi surface [31], but has the caveat that it supposes the actual existence of a Fermi surface, which can be destroyed at strong interactions.

Our goal is to construct a renormalized expansion that yields a well-behaved series, without postulating the presence of a Fermi surface. We consider the minimal renormalization scheme where the renormalized self-energy $\Sigma_R[\xi]$ is a quadratic function of the interaction ξ . See Fig. 1 for a Feynman-diagram definition. Let us discuss some possibilities for Σ_{shift} . One choice we consider is a BCS-inspired self-energy, which introduces a one-particle gap

$$\Sigma_R = \Sigma_{\text{BCS}} = \frac{\Delta^2}{i\omega_n + \gamma \xi_{\mathbf{k}}}, \quad (8)$$

where ω_n are fermionic Matsubara frequencies, $\xi_{\mathbf{k}}$ is the dispersion of the lattice, and Δ and γ are tunable parameters. Another choice is obtained from the local DMFT self-energy

$$\Sigma_R = \Sigma_{\text{DMFT}}^{\text{loc}}. \quad (9)$$

We proceed to numerical results. As a proof of principle we use the bare series as well as the BCS-shifted

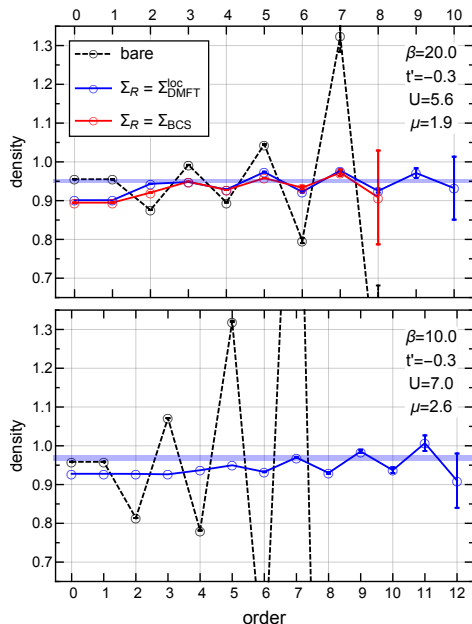


FIG. 4. Partial sums for the density in various parameter regimes are shown for the bare series (dashed black lines), the DMFT-shifted series (blue lines), the BCS-type gap shifted series (red line) and compared to the resummed DMFT-shifted series (Padé approximants, horizontal blue line).

series to compute the density and potential energy in the Hubbard atom and compare their partial sums to analytically known exact results (Fig. 2). We observe perfect convergence within 10 diagram orders of the shifted series whilst the bare series strongly diverges, to the extent that it is impossible to resum. This shortcoming of the bare series is equally true for all further examples that follow.

In Fig. 3, we compute the DMFT-shifted series in a strong-coupling, non-perturbative regime of the half-filled Hubbard model, where the bare series fails to converge as we are in the insulating regime. We are able to compute 14 orders of a convergent series that is readily resummed using Padé approximants [22, 39, 40].

In Fig. 4, we show the density at small dopings and in regimes with more immediate relevance to cuprates and pseudogap physics ($t' = -0.3$), at low-temperature and strong interaction. We compute the bare, BCS- and DMFT-shifted series and observe that the last series has the smallest Monte Carlo variance yielding 10 – 12 diagrams orders, compared to 8 orders for the first two. Both shifted series displace a negative- U singularity, associated with a superfluid transition in the attractive Hubbard model [41], further away from the origin, thus simplifying the resummation procedure [42].

One of the main motivations for this work has been the need to access the non-Fermi liquid regime of the doped square-lattice Hubbard model near half-filling. In Fig-

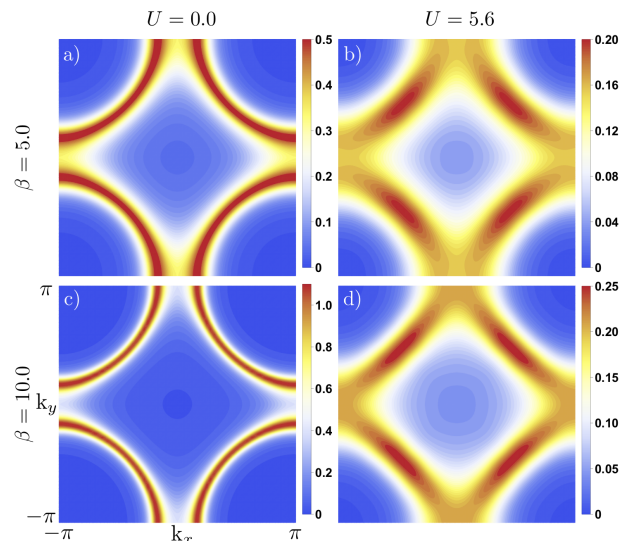


FIG. 5. Spectral function of the square-lattice Hubbard model as a function of momentum at imaginary frequency $i\pi/\beta$, density $n = 0.950(2)$ (chemical potential $\mu = 1.9$), $t' = -0.3$, $U = 5.6$, and $\beta \in \{5, 10\}$. The non-interacting system is shown for comparison.

ure 5, we show the spectral function, computed from a direct sampling of the self-energy at the lowest Matsubara frequency up to order 10 (which is expected to be a good approximation for the zero-frequency spectral function), at inverse temperature $\beta \in \{5, 10\}$ and interaction $U \in \{0, 5.6\}$. Order 6 at $\beta = 5$ and $U = 5.6$ was the limit of the bare computation of Ref. [14]. The spectral function shows significant spectral weight loss near in the antinodal region (near $(\pi, 0)$), while maintaining quasi-particle excitations in the nodal region (near $(\pi/2, \pi/2)$) and differs strongly from the the non-interacting system of same density. The results present strong deviations from the predictions of Fermi-liquid theory, compatible with the phenomenology of the pseudogap regime experimentally found in hole-doped cuprates [43]. The spectral function shows a remarkable stability as a function of temperature, signaling that the non-Fermi liquid regime is a robust feature of the doped Fermi-Hubbard model, unlike the pseudogap regime found at half-filling [28].

In conclusion, we have presented a general and efficient way to perform large-order computations for renormalized Feynman diagram series and managed to compute up to 14 expansion orders, roughly double the amount of current state-of-the-art algorithms. We have further shown that it is easy to include non-perturbative information in the construction of series expansions by using shifted propagators. We have specialized our discussion to renormalization of the one-particle propagator for the 2d Fermi-Hubbard model, where our formalism gave access to non-perturbative regimes at low-temperature and strong coupling, beyond the reach of current numerical techniques, enabling us to illustrate signatures of pseudo-

gap physics in the spectral function. Our formalism can be straightforwardly applied to the renormalization of vertex functions, necessary to access even lower temperatures where superconductivity is expected. The paradigmatic electron gas model, where the renormalization of the Coulomb interaction is necessary to define the model in the thermodynamic limit, could be another important future application. More generally, we believe that our formalism has the potential to yield significant improvements of Feynman diagrammatic computations in quantum chromodynamics, high-energy, solid-state, and statistical physics.

We thank A. Georges, M. Koivisto, O. Parcollet, and T. Schäfer for valuable discussions. This work has been supported by the Simons Foundation within the Many Electron Collaboration framework. DMFT calculations were performed with the CTHYB solver [44] of the TRIQS toolbox [45] using HPC resources from GENCI (Grant No. A0070510609). The Flatiron Institute is a division of the Simons Foundation.

-
- [1] H. A. Bethe, “The electromagnetic shift of energy levels,” *Physical Review*, vol. 72, no. 4, pp. 339–341, 1947.
- [2] S. Tomonaga, “On a relativistically invariant formulation of the quantum theory of wave,” *Progress of Theoretical Physics*, vol. 1, no. 2, pp. 27–42, 1946.
- [3] R. P. Feynman, “Spacetime approach to quantum electrodynamics,” *Physical Review*, vol. 76, no. 6, pp. 769–89, 1949.
- [4] J. Schwinger, “On quantum-electrodynamics and the magnetic moment of the electron,” *Physical Review*, vol. 73, no. 4, pp. 416–17, 1948.
- [5] R. Bouchendira, P. Cladé, S. Guellati-Khélifa, F. Nez, and F. Biraben, “New determination of the fine structure constant and test of the quantum electrodynamics,” *Phys. Rev. Lett.*, vol. 106, p. 080801, Feb 2011.
- [6] P. W. Anderson, G. Yuval, and D. R. Hamann, “Exact results in the kondo problem. ii. scaling theory, qualitatively correct solution, and some new results on one-dimensional classical statistical models,” *Phys. Rev. B*, vol. 1, pp. 4464–4473, Jun 1970.
- [7] P. W. Anderson, “A poor man derivation of scaling laws for the kondo problem,” *Journal of Physics C: Solid State Physics*, vol. 3, pp. 2436–2441, dec 1970.
- [8] K. G. Wilson and J. B. Kogut, “The Renormalization group and the epsilon expansion,” *Phys. Rept.*, vol. 12, pp. 75–199, 1974.
- [9] N. V. Prokof’ev and B. V. Svistunov, “Polaron problem by diagrammatic quantum monte carlo,” *Phys. Rev. Lett.*, vol. 81, p. 2514, 1998.
- [10] N. Prokof’ev and B. Svistunov, “Bold diagrammatic monte carlo: A generic sign-problem tolerant technique for polaron models and possibly interacting many-body problems,” vol. 77, p. 125101, 2008.
- [11] K. Van Houcke, E. Kozik, N. Prokof’ev, and B. Svistunov *Physics Procedia*, vol. 6, p. 95, 2010.
- [12] K. Van Houcke, F. Werner, E. Kozik, N. Prokof’ev, B. Svistunov, M. Ku, A. Sommer, L. Cheuk, A. Schirrotzek, and M. Zwierlein, “Feynman diagrams versus fermi-gas feynman emulator,” *Nature Physics*, vol. 8, no. 5, pp. 366–370, 2012.
- [13] Y. Deng, E. Kozik, N. V. Prokof’ev, and B. V. Svistunov, “Emergent bcs regime of the two-dimensional fermionic hubbard model: Ground-state phase diagram,” *EPL*, vol. 110, no. 5, 2015.
- [14] W. Wu, M. Ferrero, A. Georges, and E. Kozik, “Controlling feynman diagrammatic expansions: Physical nature of the pseudogap in the two-dimensional hubbard model,” *Phys. Rev. B*, vol. 96, p. 041105, Jul 2017.
- [15] K. Chen and K. Haule, “A combined variational and diagrammatic quantum monte carlo approach to the many-electron problem,” *Nature Communications*, vol. 10, no. 2725, 2019.
- [16] I. Krivenko, J. Kleinhenz, G. Cohen, and E. Gull, “Dynamics of kondo voltage splitting after a quantum quench,” *Phys. Rev. B*, vol. 100, p. 201104, Nov 2019.
- [17] J. Vucicevic and M. Ferrero, “Real-frequency diagrammatic monte carlo at finite temperature,” *arXiv preprint arXiv:1908.11826*, 2019.
- [18] A. Taheridehkordi, S. Curnoe, and J. LeBlanc, “Algorithmic matsubara integration for hubbard-like models,” *Physical Review B*, vol. 99, no. 3, p. 035120, 2019.
- [19] A. Taheridehkordi, S. Curnoe, and J. LeBlanc, “Optimal grouping of arbitrary diagrammatic expansions via analytic pole structure,” *arXiv preprint arXiv:1911.11129*, 2019.
- [20] R. Rossi, “Determinant diagrammatic monte carlo algorithm in the thermodynamic limit,” *Phys. Rev. Lett.*, vol. 119, p. 045701, Jul 2017.
- [21] A. Moutenet, W. Wu, and M. Ferrero, “Determinant monte carlo algorithms for dynamical quantities in fermionic systems,” *Phys. Rev. B*, vol. 97, p. 085117, Feb 2018.
- [22] F. Šimkovic and E. Kozik, “Determinant monte carlo for irreducible feynman diagrams in the strongly correlated regime,” *Phys. Rev. B*, vol. 100, p. 121102, Sep 2019.
- [23] R. Rossi, “Direct sampling of the self-energy with connected determinant monte carlo,” *arXiv:1802.04743*, 2018.
- [24] R. E. V. Profumo, C. Groth, L. Messio, O. Parcollet, and X. Waintal, “Quantum monte carlo for correlated out-of-equilibrium nanoelectronic devices,” *Phys. Rev. B*, vol. 91, p. 245154, Jun 2015.
- [25] C. Bertrand, S. Florens, O. Parcollet, and X. Waintal, “Reconstructing nonequilibrium regimes of quantum many-body systems from the analytical structure of perturbative expansions,” *Phys. Rev. X*, vol. 9, p. 041008, Oct 2019.
- [26] A. Boag, E. Gull, and G. Cohen, “Inclusion-exclusion principle for many-body diagrammatics,” *Phys. Rev. B*, vol. 98, p. 115152, Sep 2018.
- [27] A. Moutenet, P. Seth, M. Ferrero, and O. Parcollet, “Cancellation of vacuum diagrams and the long-time limit in out-of-equilibrium diagrammatic quantum monte carlo,” *Physical Review B*, vol. 100, no. 8, p. 085125, 2019.
- [28] F. Šimkovic, J. P. F. LeBlanc, A. J. Kim, Y. Deng, N. V. Prokof’ev, B. V. Svistunov, and E. Kozik, “Extended crossover from a fermi liquid to a quasiantiferromagnet in the half-filled 2d hubbard model,” *Phys. Rev. Lett.*, vol. 124, p. 017003, Jan 2020.
- [29] A. J. Kim, F. Šimkovic IV, and E. Kozik, “Spin

- and charge correlations across the metal-to-insulator crossover in the half-filled 2d hubbard model,” *arXiv:1905.13337*, 2019.
- [30] R. Rossi, N. Prokof’ev, B. Svistunov, K. Van Houcke, and F. Werner, “Polynomial complexity despite the fermionic sign,” *EPL*, vol. 118, no. 1, 2017.
- [31] F. Feldman, H. Knörrer, M. Salmhofer, and E. Trubowitz, “The temperature zero limit,” *Journal of Statistical Physics*, vol. 94, pp. 113–157, 1999.
- [32] A. N. Rubtsov, V. V. Savkin, and A. I. Lichtenstein, “Continuous-time quantum monte carlo method for fermions,” *Physical Review B*, vol. 72, no. 3, p. 035122, 2005.
- [33] A. Georges, G. Kotliar, W. Krauth, and M. J. Rozenberg, “Dynamical mean-field theory of strongly correlated fermion systems and the limit of infinite dimensions,” *Rev. Mod. Phys.*, vol. 68, pp. 13–125, Jan 1996.
- [34] R. Rossi, F. Werner, N. Prokof’ev, and B. Svistunov, “Shifted-action expansion and applicability of dressed diagrammatic schemes,” *Phys. Rev. B*, vol. 93, p. 161102, Apr 2016.
- [35] A. Björklund, T. Husfeldt, P. Kaski, and M. Koivisto, “Fourier meets möbius: fast subset convolution,” *Proceedings of the thirty-ninth annual ACM symposium on Theory of computing*, pp. 67–74, 2007.
- [36] This comes from the fact that the computational cost is dominated by the computations of the 2^n determinants of nilpotent polynomials of variable order.
- [37] E. Kozik, M. Ferrero, and A. Georges, “Nonexistence of the luttinger-ward functional and misleading convergence of skeleton diagrammatic series for hubbard-like models,” *Phys. Rev. Lett.*, vol. 114, p. 156402, Apr 2015.
- [38] R. Rossi and F. Werner, “Skeleton series and multivaluedness of the self-energy functional in zero space-time dimensions,” *Journal of Physics A: Mathematical and Theoretical*, vol. 48, no. 48, p. 485202, 2015.
- [39] C. Brezinski, “Extrapolation algorithms and padé approximations: a historical survey,” *Applied numerical mathematics*, vol. 20, no. 3, pp. 299–318, 1996.
- [40] P. Gonnet, S. Guttel, and L. N. Trefethen, “Robust padé approximation via svd,” *SIAM review*, vol. 55, no. 1, pp. 101–117, 2013.
- [41] T. Paiva, R. R. Dos Santos, R. Scalettar, and P. Denteneer, “Critical temperature for the two-dimensional attractive hubbard model,” *Physical Review B*, vol. 69, no. 18, p. 184501, 2004.
- [42] Unlike the bare expansion results, which is physical for all U (it is a simple U expansion), generally the renormalized results are physical only for a chosen U point. As our shift is quadratic in U , the renormalized expansion will be physical also for $-U$, where the system is in the superfluid s-wave phase at low temperature. This explains the oscillations as a function of the orders seen for both shifts: the system has a singularity at $-U$ for physical reasons, therefore the series cannot converge at U .
- [43] B. Keimer, S. A. Kivelson, M. R. Norman, S. Uchida, and J. Zaanen, “From quantum matter to high-temperature superconductivity in copper oxides,” *Nature*, vol. 518, pp. 179–186, 2015.
- [44] P. Seth, I. Krivenko, M. Ferrero, and O. Parcollet, “Triqs/cthyb: A continuous-time quantum monte carlo hybridisation expansion solver for quantum impurity problems,” *Computer Physics Communications*, vol. 200, pp. 274 – 284, 2016.
- [45] O. Parcollet, M. Ferrero, T. Ayral, H. Hafermann, I. Krivenko, L. Messio, and P. Seth, “Triqs: A toolbox for research on interacting quantum systems,” *Computer Physics Communications*, vol. 196, pp. 398–415, 2015.